PROCEEDINGS OF SPIE

SPIEDigitalLibrary.org/conference-proceedings-of-spie

Impact of a plasma mitigation process on the 266 nm pulsed LiDT of RAR nano-textured fused silica

Amile Zaaf, Hayden Small, Tadd LeRocque, Andrew Robson, Anthony Manni, et al.

Amile N. Zaaf, Hayden S Small, Tadd M. LeRocque, Andrew R. Robson, Anthony D. Manni, Douglas S. Hobbs, "Impact of a plasma mitigation process on the 266 nm pulsed LiDT of RAR nano-textured fused silica," Proc. SPIE 12300, Laser-Induced Damage in Optical Materials 2022, 123000B (2 December 2022); doi: 10.1117/12.2642768

SPIE.

Event: SPIE Laser Damage, 2022, Rochester, New York, United States

Downloaded From: https://www.spiedigitallibrary.org/conference-proceedings-of-spie on 12 Dec 2022 Terms of Use: https://www.spiedigitallibrary.org/terms-of-use

Impact of a plasma mitigation process on the 266nm pulsed LiDT of RAR Nano-Textured fused silica.

Amile N. Zaaf*, Hayden S. Small, Tadd M. LeRocque,
Andrew R. Robson, Anthony D. Manni, and Douglas S. Hobbs
TelAztec LLC, 15 A Street, Burlington, MA 01803

ABSTRACT

The pulsed laser induced damage threshold (LiDT) of Random Anti-Reflective (RAR) nano-textured fused silica optics has been shown to be many times higher than thin-film AR coated optics at wavelengths ranging from the near UV through the NIR. Because an RAR nano-texture is formed by a plasma etch process that removes part of the optic surface, the observed increase in damage resistance has kept track with the LiDT advances attained by low roughness super-polishing and damage pre-cursor mitigation techniques. In this work, nano-second pulse LiDT testing of RAR nano-textured optics was conducted at the deep UV wavelength of 266nm. The effect on 266nm LiDT of the uniform removal of additional surface material from fused silica optics using a dry plasma etch process was investigated. This plasma-polishing (PP), pre-RAR process was varied using fluorine-based chemistries that removed 100-300nm of material from each test surface, with surface roughness then characterized using white-light interferometry. Photo-thermal interferometry confirmed that no surface absorption was added by the PP, RAR, and PP-RAR plasma etching. Both standard grade, and ultra-low bulk absorption (low-OH) fused silica were included in the tests. RAR nano-textured surfaces showed an average damage threshold of 8.4 J/cm^2, a level 3 times higher than a commercially available thin-film AR coated surface. Unexpected from pulsed LiDT testing at many longer wavelengths, all plasma etched surfaces exhibited less than half the damage threshold of the untreated, as-polished fused silica surfaces, and there was no observed correlation with surface roughness or plasma etch depth. From work by others it was theorized that exposure to the deep UV photons generated by the plasma might induce absorptive electronic defects in the fused silica material that could explain the reduced damage resistance relative to non-exposed surfaces. As an initial test of this concept an RAR nano-textured sample was baked at 400C to remove the suspected electronic defect. The subsequent pulsed LiDT of this one annealed sample was found to be 15.5 J/cm^2, nearly double that of all other plasma etched samples. Further work to confirm this result is on-going.

Keywords: RAR Nano-Texture, Anti-Reflection, Motheye, 266nm LiDT, Fused Silica, Roughness, UV Absorption, Plasma Polishing

1.0 INTRODUCTION

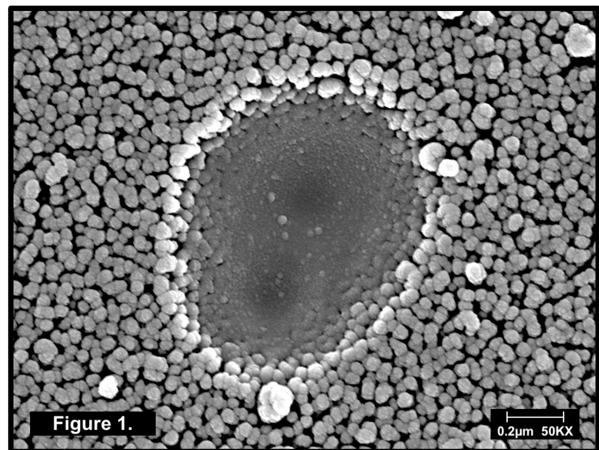

Figure 1.

The deep ultra-violet (DUV) optical wavelength of 266nm that is typically generated as the 4th harmonic of Nd-doped YAG solid state lasers, is useful for a wide range of applications such as chip and solar cell manufacturing[1-2], materials fabrication[3], chemical analysis spectroscopy[4], and scientific research into alternative energy (fusion)[5]. DUV transmitting optical materials with low absorption such as calcium fluoride (CaF_2), quartz, and synthetic fused silica (both SiO_2), are used to create lenses and other optics by subtractive manufacturing methods where after grinding to a desired shape, the optic surfaces are polished extensively to a low level of roughness and defects. It has been long established that contaminants and sub-surface cracking left over from the polishing process have the greatest impact on the resistance of the finished optic surface to damage by the ever-increasing energy available from DUV laser systems. Efforts to mitigate these damage pre-cursors through alternative polishing slurries and methods with less mechanical force[5-6], and through post

* amilenzaaf@telaztec.com; phone 1-781-229-9905; www.telaztec.com

Laser-Induced Damage in Optical Materials 2022, edited by Christopher Wren Carr,
Detlev Ristau, Carmen S. Menoni, Proc. of SPIE Vol. 12300, 123000B
© 2022 SPIE · 0277-786X · doi: 10.1117/12.2642768

Downloaded From: https://www.spiedigitallibrary.org/conference-proceedings-of-spie on 12 Dec 2022
Terms of Use: https://www.spiedigitallibrary.org/terms-of-use

polishing chemical and plasma etch techniques[7-9], have advanced the damage resistance DUV optics considerably. However, when an optic requires a further optical function such as anti-reflection (AR), conventional thin-film interference coatings introduce additional surface absorption and defects that severely limit the damage resistance to a level that is a fraction of the as-polished, or as-polished and etch mitigated optic surface[10-11].

An alternative technique of creating an AR function that does not require additional materials and accomplishes some damage pre-cursor mitigation, involves the fabrication of nano-meter scale features directly in the as-polished optic surface. A patented plasma etch process is used to controllably remove and roughen the optic surface leaving a densely packed (non-scattering) texture of randomly distributed tapered columns that serves to grade the refractive index of the surface, thereby reducing Fresnel reflection losses to extremely low levels. A scanning electron micrograph (SEM) image of such an RAR nano-texture in a fused silica window surface magnified 50,000 times is shown in Figure 1 on the right above. The crater in the center of the image is the result of standardized pulsed laser induced damage threshold (LiDT) testing as described in detail below. Because RAR nano-texturing does not introduce surface absorption, does not create concentrated electric field intensities as found with thin-film interference coatings, and does remove a significant portion of the residual polishing contaminants and sub-surface damage, the laser damage resistance of nano-textured optics has been shown to be many times higher than any type of thin-film AR coating at multiple laser wavelengths ranging from 355nm in the near UV, to 10.6µm in the long wave infrared[12-18]. In the majority of these damage tests over the past 15 years, the damage resistance of RAR nano-textured fused silica surfaces has been comparable to as-polished – or untreated (UT) - fused silica surfaces, confirming the damage pre-cursor removal concept. In this work the damage resistance of RAR nano-textured fused silica optics was determined for the important DUV wavelength of 266nm.

RAR nano-texturing of fused silica aimed at ultra-low reflection loss at 266nm results in feature sizes on the order of 30-60nm wide and 120 to 200nm deep. It is estimated that approximately 200nm of the surface is removed to leave the RAR nano-texture. In work by others investigating acid and plasma post polish damage removal processes, the estimated depth of contaminants and sub-surface cracking in fused silica ranges from 200-1000nm[5,7,9-10]. This means that additional uniform removal of surface material combined with the RAR nano-texturing process might lead to even higher laser damage resistance. Figure 2 illustrates this "plasma-polishing" (PP) concept where a reactive ion etch process similar to the RAR etch process could be used to remove more damage pre-cursors than the RAR etch alone. After the finish step in a polishing cycle, a thin smooth skin of material known as the "Bielby" layer remains at the top covering residual subsurface cracking caused by the mechanical force of the initial shaping step. The Bielby layer encapsulates impurities (shown as red dots) such as cerium and iron used in the polishing slurry. A PP etch can remove this Bielby layer along with its contaminants in a uniform manner without impacting the carefully fabricated surface shape. A similar result can be attained with a chemical etch using a mix of hydrofluoric and nitric acid, but acid etching is difficult to control and to remove material uniformly over large optic surfaces. As outlined below, several PP process variants designed to remove surface layers uniformly to various depths were first characterized by surface roughness and surface absorption measurements and then subjected to the 266nm pulsed LiDT testing.

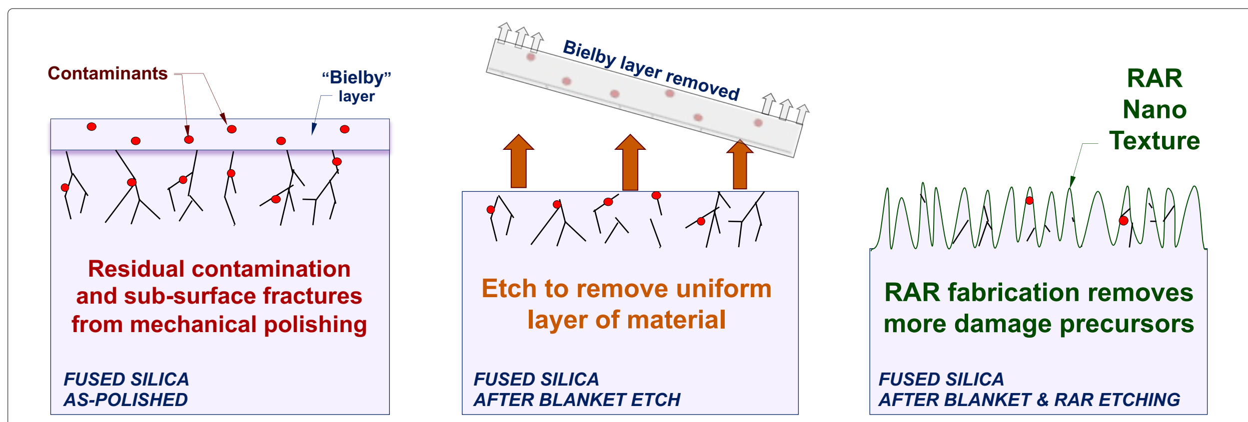

***Figure 2: Concept diagrams of the laser damage pre-cursors resulting from mechanical polishing** (left) **and the mitigation through uniform surface etching** (middle) **and subsequent RAR nano-texture fabrication** (right).*

Downloaded From: https://www.spiedigitallibrary.org/conference-proceedings-of-spie on 12 Dec 2022
Terms of Use: https://www.spiedigitallibrary.org/terms-of-use

2.0 RAR NANO-TEXTURE FABRICATION AND MEASURED PERFORMANCE

An RAR nano-texture is fabricated in a single-step dry plasma process where the gas chemistry is adjusted to provide both physical and chemical etching as well as the critical short-lived micro-masking material. The process flow is quite similar to thin-film coting deposition where optics are first thoroughly cleaned, placed into a carrier fixture, and then loaded into a vacuum chamber. Unlike coating deposition which adds alternating layers of dissimilar materials and precise thickness over the course a few hours or more, an RAR nano-texture is formed by removal of a few 100nm of the surface within just a few minutes. Typical machine cycle time from pump down through RAR etch to vent for a batch of fused silica optics is only 10 minutes, yielding a high throughput that compares favorably with even the largest thin-film deposition systems.

Figure 3 shows different views taken at 100,000 times magnification by SEM of an RAR nano-texture in the surface of a window made from Corning 7980 Grade 0A high purity UV fused silica. The carpet-like collection of features have dimensions that are much smaller than the 266nm wavelength they are intended to pass, and the features are packed together with a density that is also sub-wavelength to preclude any losses due to scattering from the texture.

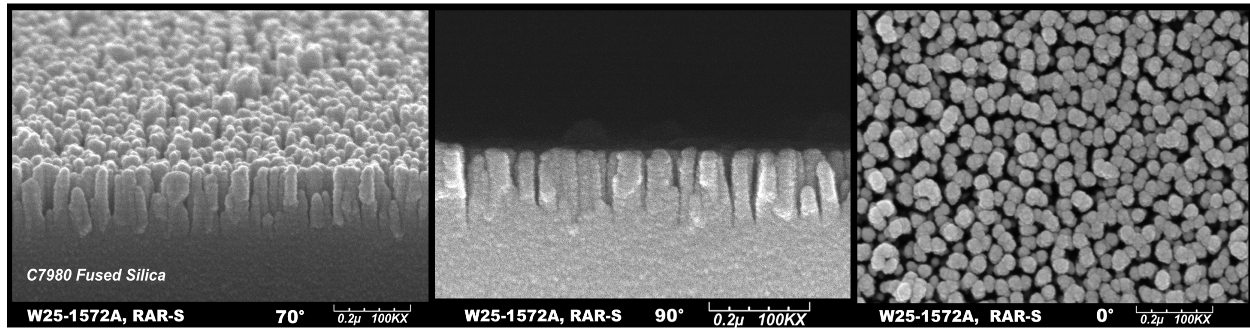

Figure 3: Elevation** (left), **profile** (middle), **and overhead** (right), **SEM images of an RAR-S nano-textured fused silica window surface at 100,000X magnification. Column features 150-200nm high are randomly distributed with <100nm spacing.

The graded-index optical function introduced by RAR nano-texturing enables unprecedented optical performance compared to thin-film AR coatings that depend on interference effects. For example the functional bandwidth of RAR nano-textured fused silica is typically 500nm for UV-VIS performance, and nearly 1000nm for VIS-NIR performance, far greater than can be achieved with even the broadest band multi-layer thin-film AR coatings (TFARCs). This bandwidth is evident in the Figure 4 image showing the visible light reflection of a TFARC fused silica window compared to an RAR nano-textured window (damage sites from the 266nm pulsed LiDT testing are evident in the lower half of the TFARC window).

Single-surface reflection losses are <0.1% over their performance band, and the texture depth and density can be adjusted for extremely low losses below 0.01% (-40dB) at specific laser wavelengths such as the typical harmonics of Yb-doped YAG at 1030/515/343/257nm. Off-axis performance is also superior, with negligible reflection change seen from +/-30°, and minimal effect from +/-60°, without the color shift that is characteristic of TFARCs.

RAR nano-textured fused silica windows prepared for the pulsed LiDT testing typically measure less than 0.1% single-surface reflection at the test wavelength of 266nm. Figure 5 shows the transmission and reflection performance of RAR nano-textured (solid green curves), and thin-film AR coated (dashed red, Thorlabs WL41050 'V'-coat design) fused silica windows prepared for this work. Note the broadband nature of the RAR nano-textured window, which shows a monotonic increase in reflection and decrease in transmission at longer wavelengths as the depth of the texture becomes small in comparison to the wavelength of light, thereby applying a smaller gradient to the refractive index. Transmission levels greater than 99.5% in the targeted wavelength ranges are routinely achieved by RAR nano-texturing due to the lack of additional surface absorption and low scatter loss. In contrast the TFARC window transmission is <98% due to the unusually high coating absorption (see section 4) measured for these commercial off-the-shelf windows.

Downloaded From: https://www.spiedigitallibrary.org/conference-proceedings-of-spie on 12 Dec 2022
Terms of Use: https://www.spiedigitallibrary.org/terms-of-use

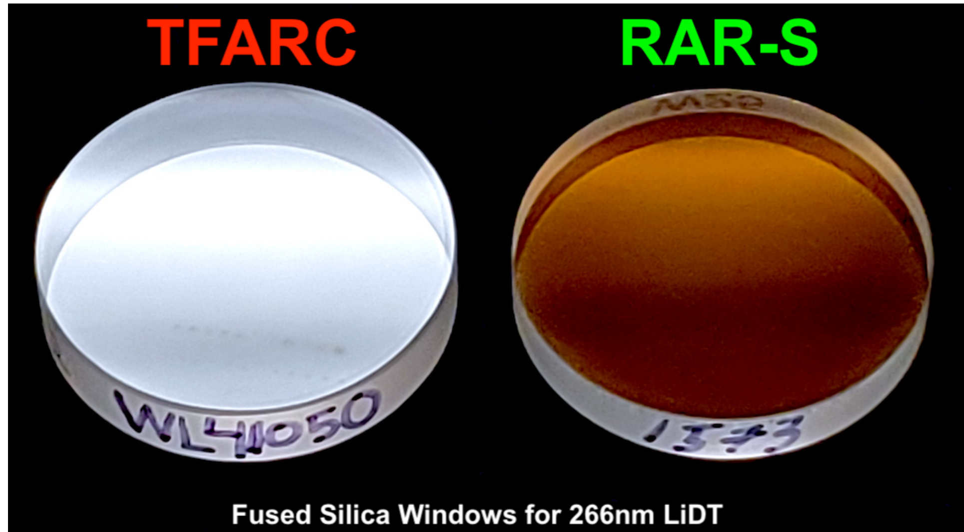

***Figure 4: Visible light appearance of an RAR nano-textured fused silica window** (right)**, and a commercial grade thin-film AR coated fused silica window with a 'V' design for 266nm** (left).*

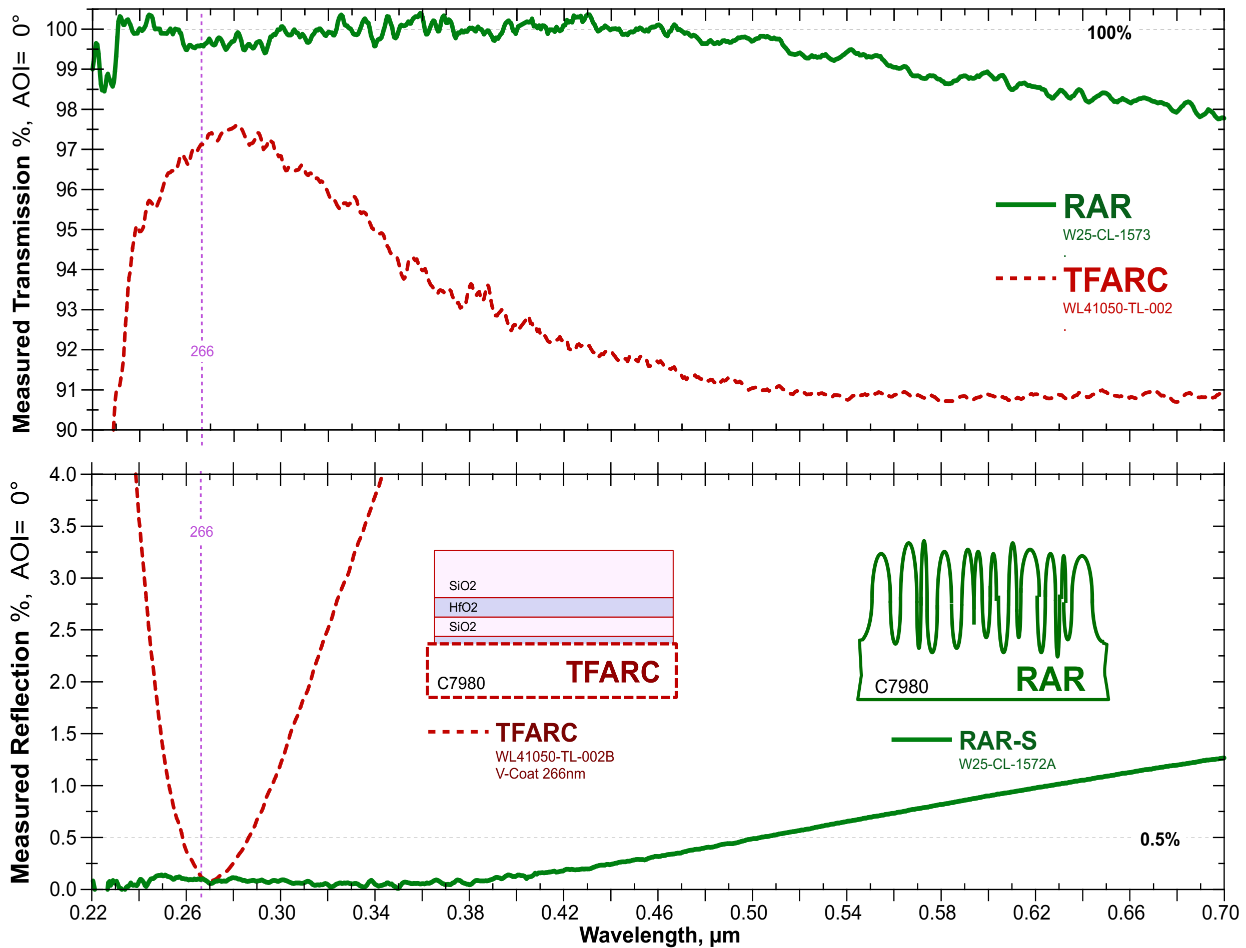

***Figure 5: Measured spectral reflection** (bot)**, and spectral transmission** (top) **of an RAR nano-textured fused silica window** (solid green curves)**, and a commercial grade thin-film AR coated fused silica window with a 'V' design** (dashed red curves).*

Downloaded From: https://www.spiedigitallibrary.org/conference-proceedings-of-spie on 12 Dec 2022
Terms of Use: https://www.spiedigitallibrary.org/terms-of-use

3.0 SURFACE ROUGHNESS MEASUREMENTS

Because it was expected that the type of etch process and the amount of surface removal developed for the PP experiments would result in greater surface roughness than the as-polished UT surfaces, a method of characterizing surface roughness was investigated. An optical surface profiling method based on interferometry with a short (1µm) coherence length LED light source was available as a service from Polytec in Hudson, Massachusetts. Polytec's TopMap Micro.View system operates with a green LED source capable of nanometer vertical resolution and 800nm lateral resolution. A 2D scan over multiple 1x1mm areas on each window surface allows an average roughness to be calculated. Such a topographical map is shown on the left in Figure 6 where the false color vertical (Z) range is over 20nm. [The green narrow band source wavelength provided some difficulty when measuring some of the PP and PP+RAR window surfaces that had very low green reflection (<0.15%), specifically samples 1581A and 1583A. A system with a red LED source would have been the better choice – in hindsight.]

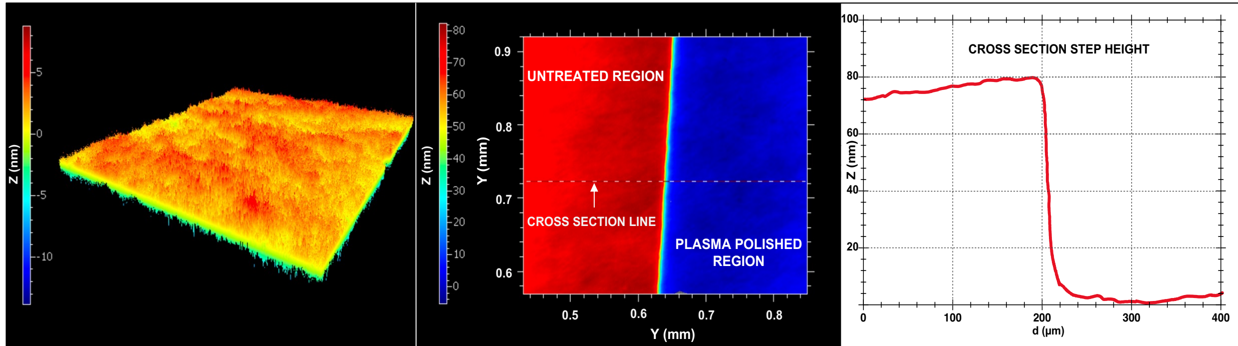

Figure 6: Surface Topography of RARPPB** (left), **step height of PPA** (middle), **and cross section step height of PPA**(right), **White light interferometry scans of topography and step height calculations of plasma polish PPA

The surface profiler was also used to determine etch depths and rates of each plasma polish recipe. PP samples were partially covered block any plasma etching of the shielded portion. The resulting step change line was visible by eye, dividing the surface into two regions as shown in the center map of Figure 6: unetched (red, covered during etching), and etched (blue region). The target etch depth was 200nm, where it was estimated that cerium and iron polishing contaminants would be removed. Multiple scans were acquired in different locations across the step, to validate step uniformity. Plasma polish recipes PPB and PP1-8 reached depths of around 210nm and 230nm respectively.

Roughness calculations were performed according to ISO 2190-2:2021 guidelines[22]. Areal root mean square roughness (Sq) was the primary variable when comparing surface roughness, which is defined as the root mean square of ordinate values within the definition area. This parameter was chosen as to acquire three-dimensional representation of the samples, as opposed to popular 2D surface roughness variables such as rms. Arithmetical mean height (Sa) and maximum height (Sz) were also calculated. Table 1 below provides all calculated surface roughness characterization values across each sample. Based on this data, no correlation was determined with PP etch depth and surface roughness which may mean that the original polish level and subsequent etching had a roughness level below the system detection threshold.

Table 1: Surface roughness and etch depth measurements

Type	UT	RAR	PPA	PPB	PP1-4	PP1-8	RAR+PPB
Roughness (Sq)	0.75	0.81	0.59	0.77	0.59	0.66	1.52
Etch Depth (nm)	-	-	83.9	209.5	112.9	231.4	-

Downloaded From: https://www.spiedigitallibrary.org/conference-proceedings-of-spie on 12 Dec 2022
Terms of Use: https://www.spiedigitallibrary.org/terms-of-use

4.0 ABSORPTION MEASUREMENTS

In this effort, several fused silica samples were RAR nano-textured for ultra-low reflection at 266nm. Absorption scans that allow separation of the surface absorption from the bulk material absorption were made at 355nm for all samples. (At the time of the initial testing, a 266nm measurement service was available, but it was thought that the 266nm laser power was insufficient to measure the low absorption fused silica samples, so a 355nm pump beam was employed with the intention of extrapolating results to 266nm.)

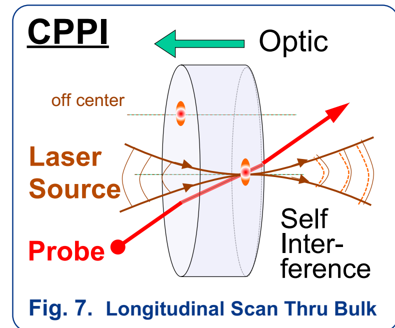

Fig. 7. Longitudinal Scan Thru Bulk

Photothermal Common-path Interferometry (PCI) services were provided by Island Interferometry and Stanford Photothermal Solutions (SPTS). As depicted in the Figure 7 diagram on the right, PCI utilizes a focused pump beam to heat the optic under test and produce a localized refractive index change following the gaussian intensity distribution of the focused spot - creating a thermal lensing effect that can be detected. A probe laser with a longer coherence length intersects the pump beam disturbance and creates a self interference pattern that amplifies the signal such that absorption levels of less the one part per million (ppm) can be observed. The stationary overlap of the two beams is scanned by moving the optic longitudinally to cross each surface.

Absorption measurements were performed on untreated (UT), RAR nano-textured, plasma polished (PP), and plasma polished then RAR textured (RAR+PP) samples. The results are given in Figures 8, 9, and 10, with bulk absorption measured in units of ppm or ppm per centimeter (ppm/cm).

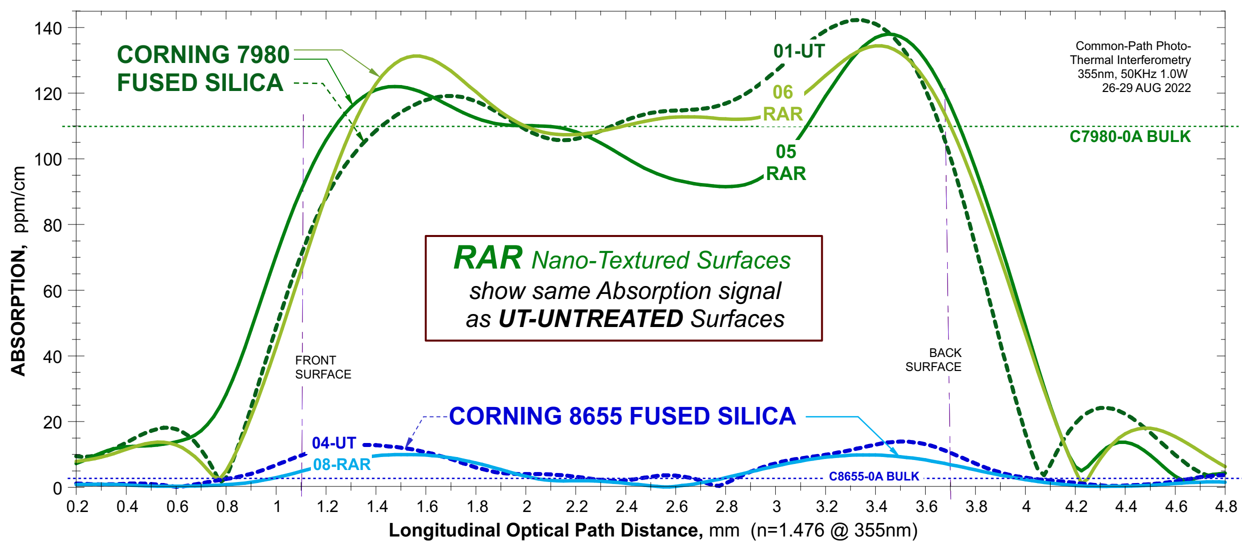

Figure 8: PCI absorption scans through as-polished *(dashed curves)* ***and RAR-nano-structured*** *(solid curves)* ***windows made from C7980 standard fused silica*** *(green, 1"Ø)* ***and C8655 low-OH fused silica*** *(blue, 0.5"Ø)* ***windows, 3.2 & 4mm thick.***

The UV-grade Corning C7980 fused silica substrates, as shown by the group of green curves in Figure 8, displayed bulk absorption values of around 110 ppm/cm when pumped by 355nm, while the low-OH content C8655 material, shown by the two blue curves, was almost immeasurable for both untreated and RAR textured samples. Note that the system has a noise floor below 1ppm/cm. In both varieties of fused silica, the RAR nano-textured surfaces showed no additional surface absorption over the as-polished surfaces, as expected. The left portion of Figure 9 below compares the absorption of a variety of plasma polished, RAR nano-textured, and untreated C7980 windows measured at 355nm. Note the large range of bulk absorption values observed in the middle of each scan is characteristic of the UV-grade material and does not correlate with the various etch processes. In contrast, on the right side of Figure 9 is the measured absorption of a Thorlabs "V-coated" C7980 window, coated on both sides, shows a large spike at one of the coated surfaces, reaching a level of 10,000 ppm. In the event that this was caused by contamination, the sample was re-cleaned before scanning again, yielding a slight decrease to 7,000 ppm shown by the surface absorption peak on the bright red curve labeled 09 TF2.

Downloaded From: https://www.spiedigitallibrary.org/conference-proceedings-of-spie on 12 Dec 2022
Terms of Use: https://www.spiedigitallibrary.org/terms-of-use

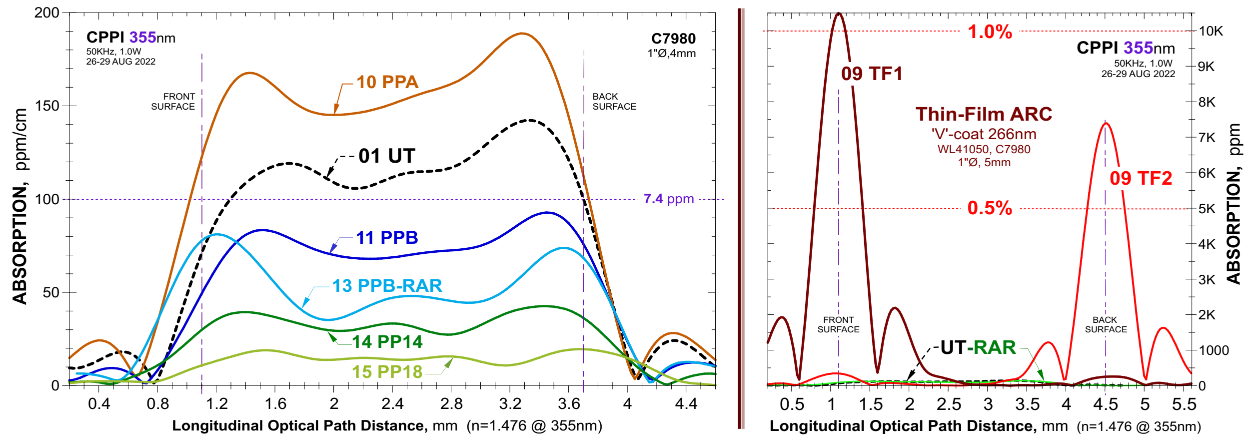

Figure 9: 355nm PCI absorption scans through plasma-polished windows (left) and TFARC windows (right).

Next, a separate set of C7980 fused silica samples was measured at 266nm at Island Interferometry, a spinout company from SPTS. This round of measurements, shown in Figure 10 was conducted in order to determine the effect of plasma-generated deep-UV radiation and thermal annealing on bulk and surface absorption[20]. The absorption traces labeled "DUV" were exposed to the same plasma as the RAR nano-textured samples, but covered with a calcium fluoride (CaF_2) window in order to chemically shield the samples while allowing them to experience high energy DUV radiation emitted by the plasma. CaF_2 was selected for its high chemical resistance and transmission in the DUV above 120nm. DUV and RAR traces labeled with "-400C" were annealed in atmosphere at 400°C for 3 hours after plasma treatment. The annealed RAR nano-textured sample was treated with the same RAR nano-texturing plasma as previous samples in Figure 6. Note that the DUV sample, which was only exposed to DUV photons, showed no increase in bulk or surface absorption over the untreated sample measured in this batch. While this implies that DUV radiation does not induce absorption, it does not rule out the potential introduction of electronic structure defects generated by VUV radiation, such as the characteristic Argon line at 50nm[21], which was absorbed by the CaF2 window during plasma exposure. Despite the lack of photo-induced absorption, annealing a DUV-exposed sample was found to increase bulk and surface absorption substantially. It is possible that annealing in atmosphere introduced a high concentration of hydroxyl groups into the surface, or allowed subsurface contamination to diffuse in a way that increased overall absorption. Both cases may be bolstered by the RAR nano-textured and annealed sample (04 RAR-400C), which possessed higher bulk absorption but lower surface absorption than the untreated sample. The lack of added surface absorption is in agreement with the concept of subsurface contamination being removed during the plasma etching process, and therefore the annealing step did not lead to elevated surface absorption in the RAR sample. Further experiments are needed to establish the cause of increased bulk absorption after thermal annealing.

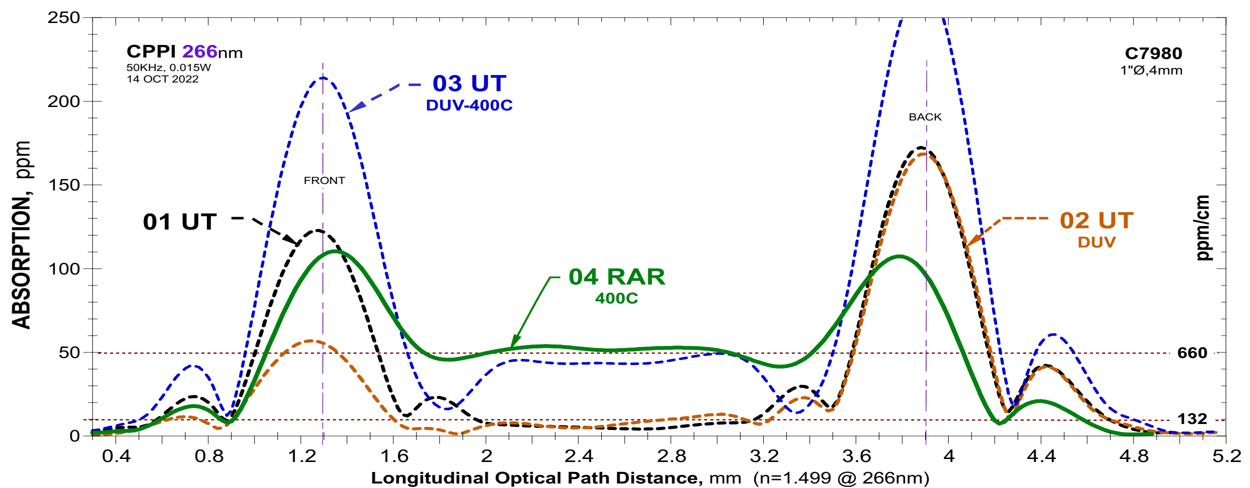

Figure 10: Longitudinal PCI absorption scans through UT, UT-DUV, DUV+400C and RAR+400C windows

Downloaded From: https://www.spiedigitallibrary.org/conference-proceedings-of-spie on 12 Dec 2022
Terms of Use: https://www.spiedigitallibrary.org/terms-of-use

5.0 PULSED LASER DAMAGE TESTING

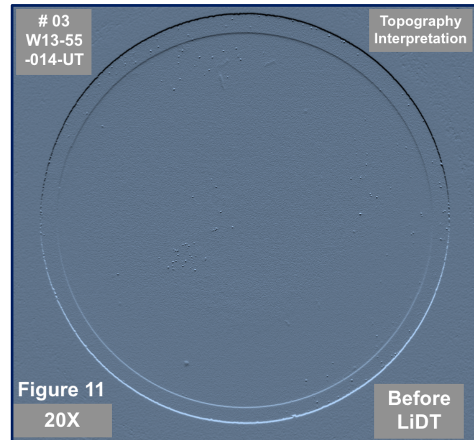

Pulsed laser damage testing was completed by Lumibird (formerly Quantel-Big Sky Laser) in Bozeman, Montana, following the ISO 21254 'S-on-1' testing protocol. Before each test, Lumibird creates a topographical map of the test surface using a low magnification inspection microscope and polarization imaging. A typical image is shown in Figure 11 on the right. Pre-existing surface defects are exaggerated by the imaging software so that such areas can be avoided during the testing. Damage testing proceeds by exposing 100 or more discrete sites to as many as 10 calibrated fluence levels per site, delivering a large number of pulses or "shots" per site. Damage is defined as any permanent change in the surface observed under 150X magnification in a Nomarski polarized microscope. The resulting damage frequency data is then plotted as a function of fluence level, with a linear fit to the data determining the threshold. The specific test configuration utilized a quadrupled Nd: YAG laser operating at the deep UV wavelength of 266nm with a pulse width of 6.6ns, 20 Hz pulse repetition rate, 210-310µm spot diameter, normal incidence, 80–150 exposure sites spaced on a grid with >2X the spot size, and 200 shots per site.

Results for three fused silica window variants – an as-polished or untreated surface (blue circles and linear fit), an RAR nano-textured surface (green triangles and fit), and a thin-film AR coated surface (red squares and fit) – are shown on the left in Figure 12. Note that with the advanced ISO 21254 protocol, many more data points are found on the slop between the no damage and 100% damage fluence levels, allowing for much improved linear fits to establish the threshold. The SEM image on the right in Figure 9 shows a damage site where a roughly circular depression is observed along with a randomly distributed set of smaller depressions within and near the exposed area. These sub-pits might be explained by residual polishing contaminants or by re-deposition of ejecta material from initial pulses that leads to further damage by subsequent pulses.

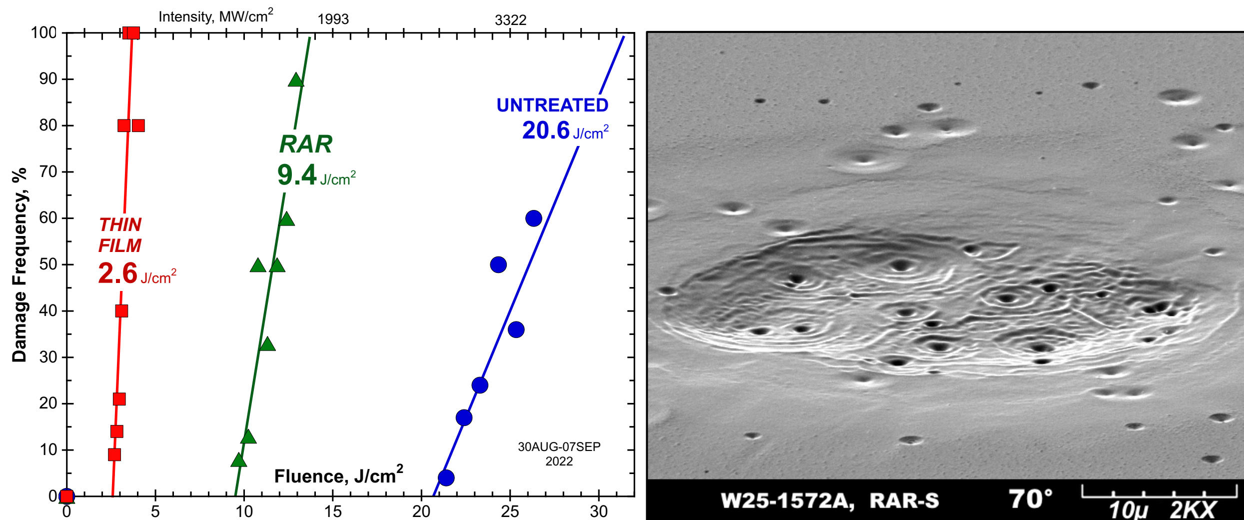

***Figure 12: Damage frequency vs. fluence level** (left)**, for three fused silica window variants after 266nm pulsed LiDT testing at Quantel. Also shown is a low magnification image of a damage site in an RAR nano-textured fused silica surface** (right).*

Figure 13 shows a bar chart comparing the damage thresholds for all windows tested. Several 1" Ø x 4mm thick fused silica windows were submitted to Quantel, these parts are labeled with the W25 prefix and are all Corning C7979-0A grade. The majority of these samples were duplicates of those sent for absorption measurements. Two 0.5" Ø x 3mm thick Corning 8655 samples were also included, designated W13. For comparison, one 1" Ø x 5mm thick thin-film AR coated window (Thorlabs W41050), optimized for 261–266nm performance, was included. Samples W25-1575 and W25-1576 served as UT controls for C7980, and W13-55-UT served as an untreated control for C8655. RAR, PP

Downloaded From: https://www.spiedigitallibrary.org/conference-proceedings-of-spie on 12 Dec 2022
Terms of Use: https://www.spiedigitallibrary.org/terms-of-use

and RAR+PP samples were also included. All of these RAR and PP C7980 samples had a comparable LiDT, and were anywhere from 2–4 times higher than the thin film coated sample. Note that any plasma treatment (PP or RAR) decreased the damage threshold significantly below that of the untreated material. In the case of the C8655 samples, the RAR nano-textured sample damaged at roughly half the fluence as that of the untreated control sample.

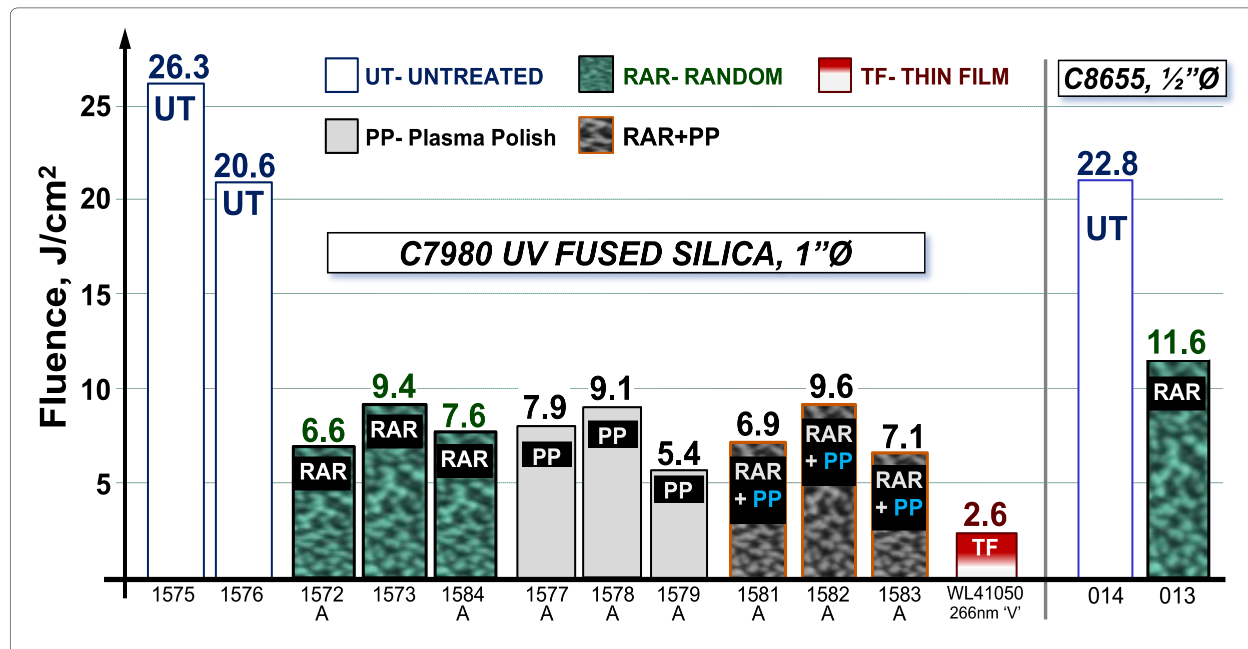

***Figure 13: Bar chart of 266nm pulsed LiDT results, all variants** (C7980 fused silica on left, C8655 fused silica on right).*

LiDT of RAR textured optics has historically reached levels near or identical to the untreated substrate, as seen in previous LiDT testing at 355nm, 532nm, 1064nm and 1538nm, but was not the case in these experiments, in which the RAR samples damaged at around half the fluence level of untreated fused silica samples. After reviewing the data in Figure 13, it was hypothesized that plasma-generated UV radiation damage may have caused the decrease in LiDT at 266nm, because there was no observable correlation between LiDT and 355nm absorption, surface roughness, or subsurface contamination removal. A group at Heraeus previously published a review of major chemical and electronic defects and their links to absorption at UV and IR wavelengths. Most relevant to this work was the non-bridging oxygen hole (NbOH) center which induces an absorption band centered at 265nm [20]. Additional groups have reported the generation of photocurrents in SiO_2 by VUV radiation below 100nm wavelengths in plasma-based manufacturing processes such as ours [21].

In order to explore this theory, four more samples of Corning 7980 material, mirroring those in the 266nm absorption measurements in Figure 10, were sent to Lumibird for further S-on-1 pulsed laser induced damage threshold tests. An untreated control (UT), DUV-exposed samples with and without thermal annealing, and an annealed RAR nano-textured (RAR+A) sample were tested. The damage threshold fluences are displayed below in Figure 14. The UT and DUV exposed samples had similar damage thresholds at 18.7 and 22.25 J/cm^2, respectively, which correlates well with their counterparts measured for 266nm absorption. Again, this implies that DUV photons of wavelengths long enough to transmit through the CaF_2 window used to block the plasma chemistry do not play a role in generating the absorptive electronic defect at 266nm, but it does not rule out the possibility that VUV-induced photocurrents are the primary sources of absorptive defects at 266nm, since the CaF_2-covered sample was not exposed to VUV radiation. Also in agreement with 266nm absorption measurements was the low damage threshold of the UT+400C sample, which was effectively untreated, aside from its exposure to DUV photons in the plasma, and annealed in atmosphere at 400°C. Finally, the annealed RAR nano-textured sample had a LiDT of 15.5 J/cm^2, nearly double that of the RAR samples which were not annealed in the first of the two LiDT experiments. Though it is only one data point, this implies the annealing step successfully recovered some of the original substrate's LiDT after plasma processing.

Downloaded From: https://www.spiedigitallibrary.org/conference-proceedings-of-spie on 12 Dec 2022
Terms of Use: https://www.spiedigitallibrary.org/terms-of-use

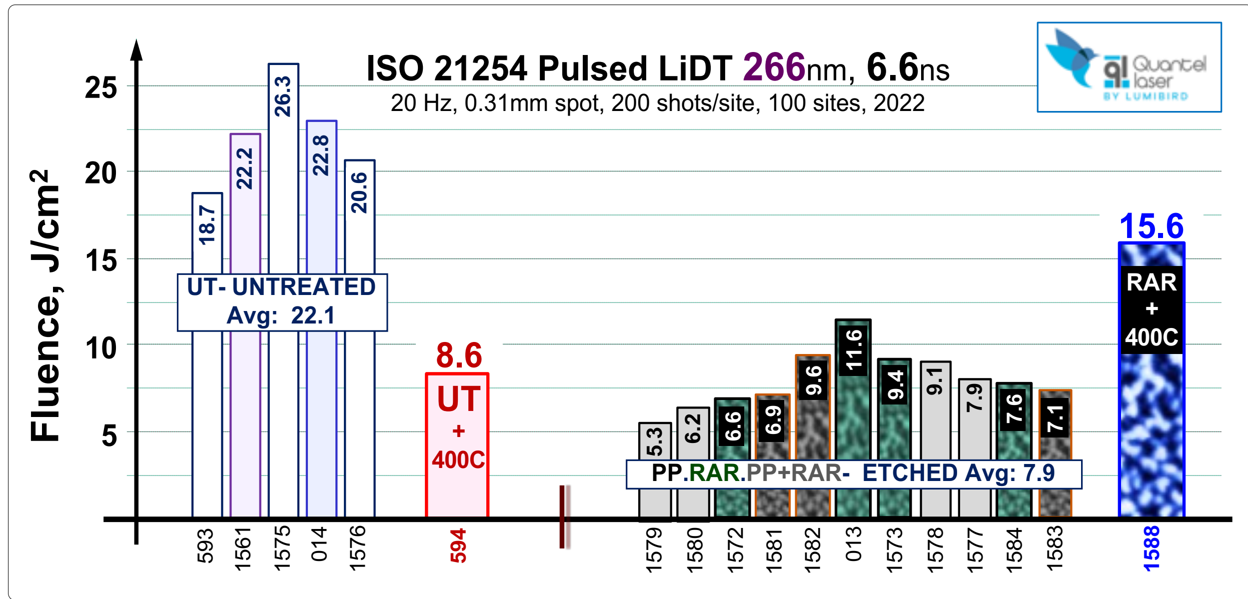

Figure 14: Bar chart of 266nm Pulsed LiDT results, all samples** (including annealed RAR, far right).**

6.0 SUMMARY

RAR fused silica optics have demonstrated superior LiDT performance over traditional thin-film AR coatings across multiple wavelengths, with 266nm being the latest included in that list. RAR can be adjusted to have an optimized wavelength at the area of interest, with samples in this discussion optimized for 266nm. Plasma polish (PP) processes were performed on untreated substrates with uniform etch depths from 100nm to 200nm. In addition, RAR nano-texturing was performed on plasma polished parts. The PP recipes utilized had no improvement on the LiDT of any of the samples.

A series of absorption tests performed at 355nm and 266nm proved that RAR introduced no additional surface absorption when compared to untreated controls. When compared to these RAR samples, the thin film anti reflective v-coating (with peak performance at 261-266nm bandwidth), the thin film demonstrated up to 10 times as much absorption for both the front and back surfaces. No level of RAR or these PP recipes introduce surface absorption in 7980 fused silica. Surface absorption at 355nm and 266nm does not explain why the RAR and PP surfaces have lower LiDT than the UT control samples. It is possible that since RAR features can reach up to 500nm, that shallow subsurface defects are already removed in a typical RAR etch, making these PP recipes redundant.

A white-light interferometer was used to scan untreated, PP, RAR, and RAR+PP parts, and surface roughness calculations were performed using Sq as the primary variable. Sq variation was only as large 1nm between all parts, which was comparable to the 0.34nm variation in the two untreated controls.

Furthermore, while there was no observed correlation between surface roughness and 266nm pulsed LiDT, any correlation that may have existed was overwhelmed by the reduction in LiDT for all plasma-etched samples, presumably due to higher bulk and surface absorption at 266nm. The LiDT of plasma polished and RAR nano-textured samples were all 3-4 times greater than that of a commercially available thin film AR coating centered at 266nm. Thermal annealing of an RAR nano-textured sample appeared to increase its damage threshold to 15.5 J/cm^2. Further studies must be conducted to provide a more statistically robust conclusion on whether electronic defects induced by VUV radiation cause increased absorption and reduced LiDT at 266nm, and what effect thermal annealing in various environments has on the 266nm LiDT of untreated and nano-textured fused silica optics.

Downloaded From: https://www.spiedigitallibrary.org/conference-proceedings-of-spie on 12 Dec 2022
Terms of Use: https://www.spiedigitallibrary.org/terms-of-use

7.0 ACKNOWLEDGEMENTS

The authors gratefully acknowledge the detailed and careful pulsed laser damage testing completed by Gary Shaffer of Lumibird (Quantel Laser), Bozeman, Montana USA. The assistance scans and calculations provided by Mario Pineda and David Damiana at Polytec in Hudson, MA were invaluable, in addition to surface metrology guidance by Dr. Christopher Brown at Worcester Polytechnic Institute, Massachusetts. Detailed and rapid PCI absorption scans and data analysis was provided through the services of Chris Franz and Dr. Alexei Alexandrovski at Island Interferometry and Stanford Photothermal Solutions (SPTS). SEM images were taken by Tyler Wozmak and John Knowles at Microvision Laboratories in Chelmsford, Massachusetts.

8.0 REFERENCES

[1] Suganuma, H., et al. "Deep-UV lithography using continuous-wave 266-nm radiation from an all solid state frequency quadrupled Nd: YAG laser." *Optical/Laser Microlithography VIII*. Proc. SPIE, **2440**, (1995)

[2] Hsiao, P-C, et.al., "266-nm ps laser ablation for copper-plated p-type selective emitter PERC silicon solar cells." *IEEE Journal of Photovoltaics* 8.4, 952-959, (2018)

[3] Egermann, J., Seeger, T., Leipertz, A., "Application of 266-nm and 355-nm Nd:YAG laser radiation for the investigation of fuel-rich sooting hydrocarbon flames by Raman scattering," Appl.Opt.**43**, 5564-5574 (2004)

[4] Sahay, P., Scherrer, S.T., Wang, C., "Measurements of the Weak UV Absorptions of Isoprene and Acetone at 261–275 nm Using Cavity Ringdown Spectroscopy for …. Breath Analyzer." Sensors **13**, 8170-8187 (2013)

[5] Neauport, J., et.al. "Polishing-induced contamination of fused silica optics and laser induced damage density at 351 nm", Optics Express, **13**, 25, 10163 (2005)

[6] Lv, L., Ma, P., Huang, J., He, X., Cai, C., and Zhu, H., "Research on laser-induced damage resistance of fused silica optics by the fluid jet polishing method," Appl.Opt.**55**, 9, 2252-2258 (2016)

[7] Neauport, J., et.al. "Characterization of the polishing-induced contamination of fused silica optics", *Journal of the American Ceramic Society*, Wiley, 100 (1), pp.96-107 (2017)

[8] Tanaka, Y., et.al., "High surface laser-induced damage threshold of SrB_4O_7 single crystals under 266-nm (DUV) laser irradiation", Optics Express, **28**, 20, 29239 (2020)

[9] Chen, J., Cheng, X., Wu, L., Wei, C., and Shao, J., "Research on competition evolution for increasing damage threshold of fused silica by atmospheric pressure plasma processing." Opt. Engineering, 61(6), 063101 (2022)

[10] Cho, B., Lyu, A., and Feldman, M. "Laser induced damage resistance of 266nm AR coatings" *Laser-Induced Damage in Optical Materials: 2013,* Proc. SPIE **8885**, 888524-1-9 (2013)

[11] 266nm Pulsed LiDT of commercial thin-film AR coatings;
https://www.edmundoptics.com/p/20mm-dia-266nm-laser-v-coat-lambda20-fused-silica-window/20381/ (3J/cm^2, 20ns)
https://www.thorlabs.com/newgrouppage9.cfm?objectgroup_id=1121 (2J/cm^2, 10ns)

[12] Lowdermilk, W. H., Milam, D., "Graded-index antireflection…., " Appl. Physics Letters, **36** (11), 891 (1980)

[13] Hobbs, D.S., MacLeod, B. D., "High laser damage…. micro-structures.., " Proc. SPIE, **6720**, 67200L (2007)

[14] Hobbs, D.S., et.al., "Contamination resistant antireflection nano-texture.., " Proc. SPIE, **8885**, 88850J (2013)

[15] Siddique, R.H., Gomard, G., Hölscher, H., "The role of random nanostructures for the omnidirectional anti-reflection properties of the glasswing butterfly", Nature Communications, **7909**, 6:6909 (2015)

[16] MacLeod, B.D., et al. "CW laser damage testing of RAR nano-textured fused silica and YAG." *Laser-Induced Damage in Optical Materials 2017*. Proc. SPIE **10447**, 10447-1, (2017)

[17] Hobbs, D.S., et.al, "Pulsed laser damage resistance of nanostructured high reflectors for 1064nm" *Laser-Induced Damage in Optical Materials: 2018,* Proc. SPIE **10805,** 108051E-1 (2018)

[18] Gadamsetti, P., and Poutous, M.K., "Fresnel reflection suppression from deterministic illumination diffusers using antireflection random nanostructures." Opt. Engineering, **61**(6), 063106 (2022)

[19] Alexandrovski, A., et. al., "Photothermal common-path interferometry….." Proc. SPIE **7193**, 71930D (2009)

[20] Nürnberg, F., et.al. "Bulk damage and absorption in fused silica due to high-power laser applications." *Laser-Induced Damage in Optical Materials: 2015*. Proc. SPIE, **9632,** (2015)

[21] Okigawa, M, et.al. "Reduction of ultra-violet-radiation induced damage ….." *7th International Symposium on Plasma-and Process-Induced Damage*. IEEE, (2002).

[22] International Organization for Standardization (2021). *GPS Surface texture: Profile Part 2: Terms, definitions surface texture parameters* (**ISO 21920-2:2021**). https://www.iso.org/obp/ui/#iso:std:iso:21920:-2:ed-1:v2:en

Downloaded From: https://www.spiedigitallibrary.org/conference-proceedings-of-spie on 12 Dec 2022
Terms of Use: https://www.spiedigitallibrary.org/terms-of-use